Float Design to Limit Displacement in Severe Seas

Stallard, T., Stansby, P.K., Weller, S.D. and Williamson, A.C.[1]

[1]Joule Centre, School of Mechanical, Aerospace and Civil Engineering
University of Manchester, Manchester, UK
E-mail: tim.stallard@manchester.ac.uk

Abstract

Many studies have been published concerning the influence of the immersed shape (in still water) of a floating body on its response and power capture from ocean waves. With a few notable exceptions, much of this analysis has assumed small amplitude motion and linear models have been employed to predict response. The form of the upper surface of such a body has received little attention. Here, it is shown that the upper (top) surface of a floating body can be designed to ensure that the response amplitude of the body is within a specified value. This is of considerable importance to the survivability of wave energy devices. The approach used is to affect a large increase of both natural period and hydrodynamic damping for only a small change of float mass. These two factors impose a hydrodynamic limit on the displacement which may be exploited to avoid the 'end-stop' problem often encountered in wave device design. To demonstrate the change of response, experimental measurements are presented of the response of an axisymmetric float with rounded base and conical upper surface with rounded perimeter due to a range of regular, irregular and focused wave conditions. Power extraction is not considered since the mechanically undamped response represents the worst case. In contrast to a simple, straight-sided axisymmetric float, a smaller change of mass is required to satisfy a particular response amplitude limit. Although a significant reduction is not expected, hydrodynamic damping may reduce with increasing physical scale and this remains to be quantified.

Keywords: Wave Energy, Heave Motion, Survivability, Extreme Waves

Nomenclature

A_j	=	Added mass in mode j (kg)
B_j	=	Radiation damping in mode j (Ns/m)
F_j	=	Excitation force in mode j (N)
H	=	Height of pulley axis above MWL (m)
H_s	=	Significant wave height (m)
M	=	Total mass (kg)
S	=	Stiffness (N/m)
T_{n}	=	Natural period (s)
T_{p}	=	Peak period of sea-state (s)
V	=	Displaced volume (m^3)
a	=	Float radius
a_0	=	Float radius at water plane ($z = 0$)
a_m	=	Measured wave amplitude (m)
f	=	frequency (Hz)
k	=	Wavenumber satisfying linear dispersion relation (m^{-1})
m_d, m_c	=	Displaced mass (ρV) and counterweight mass
r_p	=	Radius of pulley (m)
x	=	Horizontal ordinate (+ve in wave-direction)
z	=	Vertical ordinate or displacement (+ve upward)
β	=	Angle of supporting cable from vertical ($^{\mathrm{O}}$)
ϕ	=	Angular displacement (rad)
ω	=	Angular frequency (rads^{-1})
Suffixes		
imm	=	mean immersion (free surface to base of cone)
j	=	mode: 1=surge, 3=heave
m	=	measured

1 Introduction

One of the most onerous design problems faced by wave energy device developers is the disparity between the loads during normal operating conditions and those during severe storm conditions. In many cases, designers must ensure that the peak-to-peak oscillation of a device is within a finite range set by structural or mechanical constraints such as the dimensions of the supporting structure or the stroke of the generator. Operational and extreme conditions vary with deployment site but, as a broad approximation, operating conditions are wave-fields with peak periods in the range $T_{\mathrm{p}} \sim 6-10$ s and significant wave heights $H_s < 5$ m whereas extreme conditions can be considered as sea-states with $T_{\mathrm{p}} > 12$ s and $H_s > 6$ m (and in some cases up to 10 m). Within a fully developed wave-field, extreme waves may occur with a wave height (trough-crest) more than double the significant wave height; these represent a peak-load design condition for fixed offshore structures. To be economically viable, wave devices must generate useful output in the wide range of operating conditions expected at the design site whilst also surviving extreme conditions. Many heaving wave energy devices comprise a buoyant (approximately) cylindrical float whose oscillation drives a power take-off system. These devices may be taut moored (AWS, CETO), slack moored (OPT Powerbuoy, Aquabuoy, Wavebob, WaveSync) or supported from a larger fixed or buoyant structure (FO^3 Buldra, Wavestar, Trident, Manchester Bobber). Information on particular wave energy devices can be obtained from company websites and in technology reviews (e.g. [1]).

For all these systems, the maximum device motion during a wave-cycle must be within a finite limit imposed either by the generator stroke or by the structure dimensions. Individual devices in this category are typically termed point absorbers [2] and the float form and dimensions are selected to optimise annual electrical output from the wave conditions expected at the deployment site. To optimise power output from an oscillating wave energy device the float velocity must be in phase with the excitation force and mechanical damping must be similar to radiation damping [2]. For a regular wave of a particular frequency the phase condition is satisfied by matching device natural frequency to incident wave frequency. In theory this can be achieved in irregular waves by applying conjugate control [3]. In practice it is impossible to achieve optimal response in irregular waves but various sub-optimal control methods such as latching [2, 4, 5] have been proposed that are designed to minimise the phase difference between velocity and excitation force, at least while the magnitude of the force is large. In general, a condition for implementing this type of wave-by-wave control is that the natural frequency of the float is greater than the incident wave frequency (device natural period less than wave period).

The design natural period for a device is therefore in the range 5 - 7 s (e.g. [6]) and typical float dimensions are of the order of 4-6 m radius ($F0^3$ 4 m, Manchester Bobber 5 m, Wavestar 5 m, AWS Pilot Plant 4.25 m) and, particularly for structure-supported devices, the draft may be similar. To maximise power capture, response amplitude ratios (ratio of float displacement to wave amplitude) greater than unity are required and so float motions of the order of 10 m may occur during operational conditions. For economic reasons it is desirable to ensure that this excursion is not exceeded, even in severe conditions with significant wave heights of 5-6 m. Since the effects of extreme loads must be considered in conjunction with failure modes, the provision of an external force to limit motion may not always be possible. To limit the mechanically undamped response of a heaving wave energy device either natural period and/or damping must be adjusted. Adjustment of natural period can be employed to tune response (attain optimal amplitude) in operating conditions or to de-tune the device to limit response in severe wave conditions. For the simple configuration of a heaving buoy, natural period is dependent on water plane area and system mass. Of the two, it is generally more straightforward to adjust the system mass. However, although an immersed form can be identified that optimises power capture for a given immersed volume and excitation frequency [7], the large changes of mass required to modify the natural period over a useful range are difficult to achieve in practice. Furthermore, even though response amplitude of a heaving float will reduce as the wave period increases relative to natural period, the amplitude ratio only reduces to unity unless damping is significantly increased. It is therefore advantageous to investigate methods for limiting the response amplitude of a float that do not rely on either change of mass or mechanical damping.

For power output a shallow draft float is required with a natural period around 20% less than the peak wave period. However, the float geometries that operate effectively in these conditions may experience large motions during extreme conditions. These conditions may correspond to a power take off failure mode, increase of mechanical damping may not be possible and it is therefore desirable to limit motion hydrodynamically. This can be achieved by selecting a shape whose response characteristics can be adjusted by only a small change of mass. A feasible form is identified by considering the draft variation of hydrodynamic parameters obtained using linear analysis (WAMIT [8]). Since numerical models for simulating the non-linear response of a wave device are not extensively validated, particularly for extreme conditions, an experimental approach is employed for the remainder of the study. Experimental measurements, at approximately $1:68^{\text{th}}$ scale, are presented of float motion during regular, random and focused waves to demonstrate the influence of a small change of draft on the maximum excursion. There is no power generation in this investigation since this would reduce motion and hence would not represent the worst case response.

2 Float Form

The motion of the wave-activated part of a heaving device is often analysed assuming linear wave forcing and small amplitude response [2, 9]. This approach can be extended to allow simulation of time-varying response to irregular waves (reviewed in [10]). An underlying assumption is that the immersed volume of the device does not change either between individual sea-states (with different peak frequency) or during response to a particular incident wavetrain. In part this is due to difficulties associated with changing the immersed volume. Assuming small amplitude motion, the natural frequency of an oscillating float can be estimated as $\omega_n = (S/M)^{1/2}$ where S denotes the hydrostatic stiffness and M the total system mass. Assuming small amplitude oscillation in heave, the hydrostatic stiffness is proportional to the water plane area ($\rho g \pi {a_0}^2$ for an axisymmetric body of radius a_0 at the waterline) whilst for oscillation in surge or sway an external restoring spring must be provided. For an axisymmetric body in heave, natural frequency is therefore proportional to the water plane radius (a_0) and to $M^{-1/2}$. For a straight sided device, the hydrostatic stiffness is constant with draft and so a large change of mass is required to change natural period. (For example, the mass and draft of a neutrally buoyant hemispherical ended cylindrical float must be increased by 400 Tonnes and nearly 5 m to increase the natural period from 7 to 9 s.) This is difficult to achieve in practice.

A large change of response could be achieved by selecting a float form such as that shown in cross-section in the left hand frame of Figure 1 comprising two cylindrical sections connected by a smooth transition. In comparison to a straight sided cylinder (shown dashed), the hydrostatic stiffness, displaced mass and hence natural period are nonlinear with draft and so a large reduction of water plane area and small increase of displaced mass occur if the draft is increased from near the top of the straight sided section to above the conical section. Here, the upper cylinder (or stem) radius is one-third that of the lower cylinder and the upper surface is inclined at 30$^{\rm o}$ and so this change of draft requires only a small change of float mass (approx. 10% of the displaced mass).

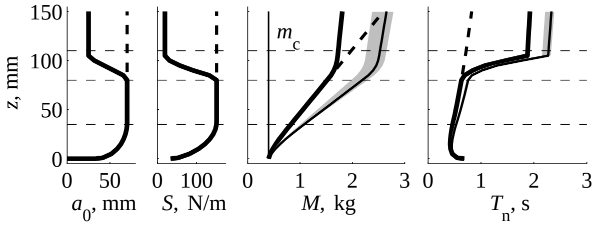

Figure 1: Draft-variation of water plane radius (a_0), rate of change of buoyancy force (S), and both float mass (M=displaced mass + counterweight mass) and indicative range of added mass (shaded). Round ended cylinder with straight sides and conical top. Radius of lower section is $a = 74$ mm, radius of upper section is $a = 25$ mm. Variation of natural period ($T_{\rm n} = 2\pi(M/S)^{1/2}$ assuming small amplitude response) also shown. Drafts of 35, 80 and 110 mm are indicated.

For power generation, the (still) waterline would be within the straight-sided cylindrical part of the float such that the wetted volume is a round-ended cylinder (35-85 mm draft). Response in this range is expected to be nearly linear with wave amplitude, at least until the response amplitude ratio is sufficiently large to immerse the upper surface during part of a wave-cycle. Similar forms (including hemisperical ended cylinders and hemispheres which have similar hydrodynamic characteristics, see Figure 2) have been shown to be suitable for power generation and have been widely studied. Heave excitation force and radiation damping reduce with increasing draft and so (providing mass can be adjusted) it is beneficial to increase draft with increasing wave period to maximise power output. However, these forms become less suitable in long waves since the undamped heave response amplitude will be large and there is no restoring force, and minimal damping, limiting excitation in surge (see B_1 in Figure 2(b)).

When the upper surface is completely immersed (e.g. 110 mm draft) such that the (still) waterline is within the narrow cylindrical part of the float, the small amplitude natural period is increased significantly due to a reduction of water plane area (Figure 1) and an increase of added mass (Figure 2(a)). Furthermore, both the heave excitation force and radiation damping are reduced to a fraction of those on a round-ended cylinder (Figure 2(c)). This form would obviously not be an efficient wave energy converter since radiation damping in heave is small ($B_3 \sim 0$) and linear analysis implies that large response amplitude ratios would occur. However, it is reasonable to expect that when the upper surface is immersed to a shallow depth there will be significant additional forces on the body due to non-linearity of the free surface, wave sloshing and breaking and viscous effects. These phenomena are not straightforward to simulate and so the behaviour of this float is studied experimentally.

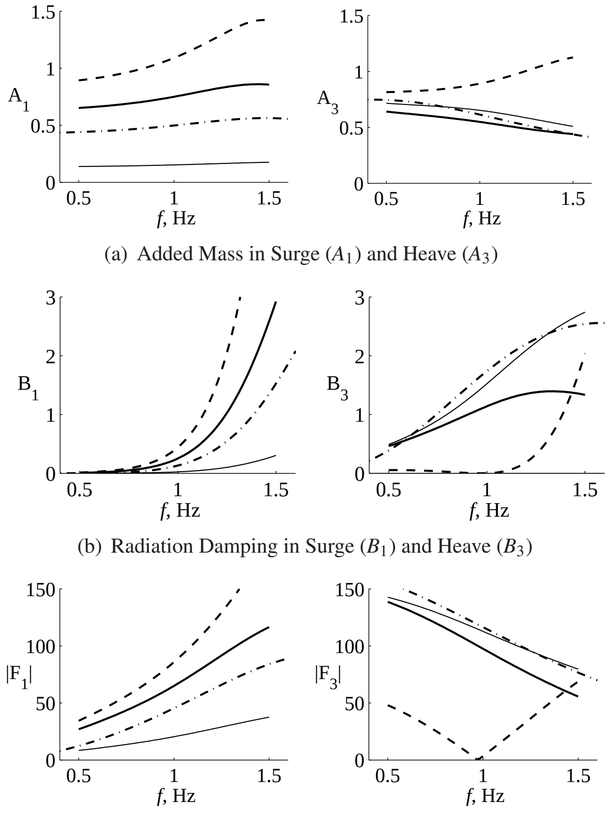

(a) Added Mass in Surge (A_1) and Heave (A_3)

(b) Radiation Damping in Surge (B_1) and Heave (B_3)

(c) Excitation Force in Surge (F_1) and Heave (F_3)

Figure 2: Hydrodynamic parameters for axisymmetric float at drafts of 35 mm (thin solid line), 85 mm (thick solid curve) and 110 mm (thick dashed curve) obtained from linear diffraction analysis (using WAMIT) of the geometry shown in Figure 1. Parameters for hemispherical float of radius equal to lower cylindrical section also shown (dash-dot).

3 Experimental Arrangement

The wave conditions considered are periods between 8 and 12 s full-scale, regular wave amplitudes up to 4.75 m, focused waves with height of 10 m and irregular wave fields with significant wave heights up to 10 m. Although not the most extreme conditions that can occur, 8 s period is representative of operating conditions whilst 12 s period represents North Sea storm conditions [11]. Tests were conducted in the 5 m wide wave and current flume at the Univeristy of Manchester which has a flat bed of length 18.5 m from paddles to mid-beach. A constant water depth of 0.45 m was used representing 30 m depth at 1:68$^{\text{th}}$ geometric scale and so the wave frequencies studied are in the range 1.063 Hz to 0.688 Hz with regular wave amplitudes up to 70 mm. In all tests, the float was located at a distance $x_0 = 3.6$ m from a set of Edinburgh Designs wave-paddles and at the centreline of the flume (i.e. 2.5 m from both tank walls). For this channel width, float response due to wave frequencies greater than 0.4 Hz can be assumed to be representative of the unconstrained case (this ensures that wavelength$< D_c$ where D_c the channel width [12, 13]).

A pulley-supported float (Figure 3), radius $a = 0.074$ m, is employed such that the total oscillating mass comprises three components; the displaced mass ($m_d = \rho V$), frequency dependent added mass ($A_3(\omega)$) and supplementary mass ($2m_c$). In contrast to a neutrally buoyant system this allows variation of total system mass without change of immersed volume and added mass (i.e. without change of m_d or A_3). Alternatively, draft may be adjusted without change of total system mass. A similar approach is described in [14] although in the present arrangement the counterweight provides an upward force on the float that varies with counterweight inertia rather than applying downward force through a supporting strut. Three float drafts are studied as summarised in Table 1 and corresponding to the drafts indicated on Figure 1. A fourth configuration (Max$^{(2)}$) is discussed in Section 4.2. The natural period listed for each configuration is calculated assuming small amplitude motion and using hydrodynamic parameters obtained by linear analysis (conducted using WAMIT [8]), Figure 2. A nominal natural period of the system is given as $T_n = (S/M)^{1/2}$ where $M = m_d + 2m_c + A_3$ although it is recognised that the actual value may be somewhat different due to non-linear response. Of course, this approach is only valid as the response amplitude approaches zero and the hydrodynamic parameters are not expected to be exact for the max-draft case for which the inclined upper surface is very close to the free-surface. However, since this information is straightforward to obtain these values provide a useful measure for comparison and future evaluation of model performance. For two cases (min- and mid-draft), the natural period is smaller than the incident wave periods considered and so phase control strategies could be employed to improve output; these configurations represent the lower and upper bounds to the typical operating range of a nominal device. To represent the worst case in terms of response amplitude, the natural period when the conical top of the float is immersed is close to that of the low frequency waves tested.

Float response is measured relative to the axis of the supporting pulley and defined as $z' = \phi r_p$ where ϕ is the angular displacement of the supporting pulley of radius $r_p = 17.5$ mm. Since the horizontal displacement is less than one radii in all cases considered z' is a reasonable approximation to the true vertical displacement, z. (By geometry, $z = z' \cos\beta$ where $\beta = \tan^{-1}(x/(H-z))$ is the angle of the supporting cable to the vertical when the float is displaced by distance x, so for $x < a$, $\beta < 6^{\circ}$ and $z \sim z'(1 \pm 0.005)$). Angular displacement is measured using a HEDS9000 quadrature encoder reading an HEDM 6120 T12 code wheel that provides position measurement to within 0.2°. Wave elevations are measured at 0.9 m upwave (3 gauges), in-line (1 gauge) and 0.9 m downwave (3 gauges) of the float using capacitance type wave gauges and all data is sampled at 256 Hz. In the following, the suffix m denotes wave conditions measured in the absence of the device. Measurements of device response are synchronised to the incident wave by matching wave measurements from the upwave gauges taken with- and without the float installed.

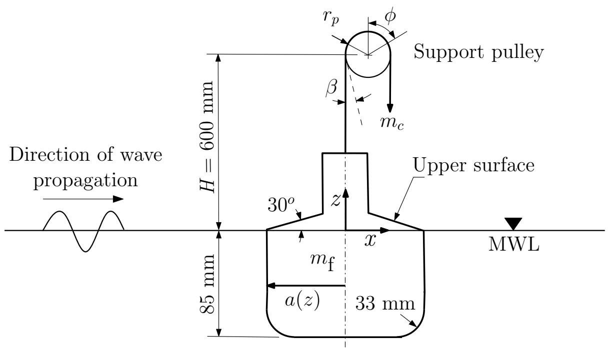

Figure 3: Experimental arrangement of single axisymmetric float at mid-draft indicating key dimensions and co-ordinate system (x +ve in direction of wave propagation, z +ve upward). Float mass ($m_f = m_d + m_c$) is altered to change draft.

	Draft (mm)	a_0 (mm)	m_c (kg)	m_f (kg)	A_3 (kg)	M_T (kg)	T_n (s)
Min-	35	75	0.40	0.82	0.67	1.22	0.65
Mid-	85	75	0.40	1.58	0.58	1.98	0.75
Max-	110	45	0.40	1.74	0.82	2.14	1.35
Max$^{(2)}$	110	45	0.24	1.58	0.82	1.82	1.28

Table 1: Float mass, counterweight and ballast employed for draft of 35, 85 or 110 mm in still-water. Natural period (T_n) is estimated assuming small amplitude response for $f_w = 0.766$ Hz using added mass coefficients obtained from hydrodynamic analysis of the corresponding float geometry using WAMIT (see Figure 2). Note that 0.15 kg $\sim$ 50 Tonnes, 0.40 kg $\sim$ 125 Tonnes and 1.58 kg $\sim$ 500 Tonnes at 1:68$^{\text{th}}$ geometric scale.

4 Measured Response

Initially the linearity of response amplitude is discussed to demonstrate the significant change of behaviour due to the immersion of the upper surface. Subsequently measurements are presented of the time-varying response to focused wave groups and to irregular wavefields.

4.1 Regular Waves

The influence of changing the float draft can be clearly seen by considering the linearity of response amplitude with wave amplitude. Figure 4 shows the variation of response amplitude ratio (z_m/a_m) with incident wave amplitude (a_m) for each float for three wave frequencues corresponding to full-scale periods of approximately 8, 11 and 12 s. When ballasted to the shallow draft position, the float attains response amplitudes greater than the incident wave amplitude over a range of wave frequencies. Response amplitude varies (nearly) linearly with incident wave amplitude for the three conditions shown with amplitude ratio increasing as a resonant response is approached (as wave period exceeds 1.0 Hz, see inset to Figure 4(b)). Maximum response amplitudes for this float are observed at frequencies close to 1.3 Hz (not shown). Note that, for this case, measurements are only presented up to an absolute displacement of approximately 40 mm since the float separates from the free surface at larger amplitudes. When the float is ballasted to intermediate draft, response amplitude ratio is constant for all wave amplitudes (ratio of between 1.2 and 1.3) whilst wave frequency is lower than the natural frequency (Figure 4(a)). However, when response is near-resonant (e.g. $f_w = 1.06$ Hz, $f_n \sim 1.3$ Hz) the variation of response amplitude is clearly nonlinear. For wave amplitudes less than 21 mm, float response amplitude is close to double the wave amplitude but this decreases with increasing wave amplitude towards an amplitude ratio of 0.8 at $a_m > 60$ mm. Effectively the absolute response amplitude remains at a (nearly) constant value of between 46 and 50 mm over this range. As will be seen, the onset of this response limit can be attributed to the immersion of the upper surface of the float during part of the wave cycle. For the max-draft case (Figure 4(b)), response is consistently less than 65% of the incident wave and the response amplitude undergoes nonlinear variation with wave amplitude. Larger responses are measured at a lower wave frequency (0.688 Hz) since this is closer to the natural frequency of the float (estimated as 0.74 Hz). For this frequency, response amplitude ratio increases up to 0.65 at 42 mm wave amplitude and subsequently decreases to 0.5 at wave amplitudes greater than 65 mm. At 0.766 Hz, response amplitude ratio increases to approximately 0.3 at wave amplitude of 25 mm and response amplitude remains approximately constant with increasing wave amplitude ($z_m/a_m \sim 0.3$ for $30 < a_m < 70$). At 30 mm amplitude, mean displacement is 17 mm (0.766 Hz). At 0.766 Hz, max-draft response amplitude ratio increases roughly linearly with incident wave amplitude ($z_m/a_m = 1.15$ to 1.4 over the range 13 to 70 mm ampltude).

An important observation from these tests is that as the wave amplitude is increased, the mean immersion of the upper surface of the float increases from its position in still water (Figures 5 and 6(d)). For the mid-draft position, change of immersion is dependent on the incident wave frequency, and significant change of immersion is

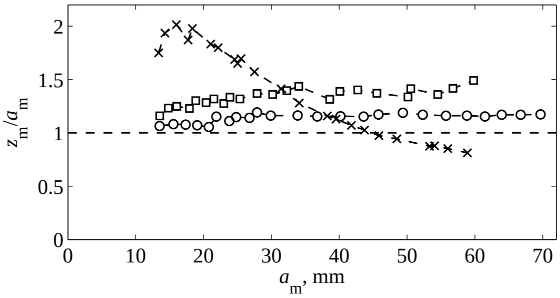

(a) Float draft = 85 mm, float mass = 1.58 kg

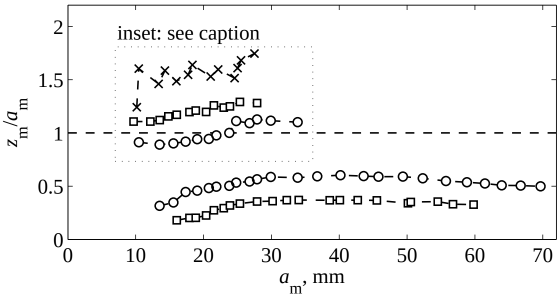

(b) Float draft = 110 mm, float mass = 1.74 kg

Figure 4: Measured response amplitude (z_m/a_m) of (a) mid-draft float and (b) max-draft float due to incident wave frequencies of 0.688 Hz (circle; $T \sim 12$ s), 0.844 Hz (square; $T \sim 10$ s) and 1.063 Hz (cross; $T \sim 8$ s). Response amplitude of min-draft float also shown as inset to (b). Masses used for each draft are listed in Table 1. Dashed line indicates unit response amplitude.

observed when the wave frequency is 1.063 Hz. For lower frequencies, ($f < 0.844$), the mean displacement remains close to zero for wave amplitudes less than 55 mm but increases slightly in larger waves. In these conditions, the response amplitude is close to the draft of the float (75 mm). For the high frequency waves, immersion remains close to zero only for small wave amplitudes ($a < 20$ mm). Subsequently the mean displacement increases with incident wave amplitude towards a limit of approximately 30 mm. It is clear that this increase of immersion causes the reduction of response amplitude ratio observed for this float in Figure 4(a); response amplitude ratio reduces from 1.8 to 0.8 as the wave amplitude increases from 20 to 60 mm and the mean immersion increases from 0 to 30 mm.

For the max-draft float, the upper surface (i.e. base of the cone) is immersed by 27 mm when at rest but the mean immersion increases towards a limit of close to the wave amplitude (immersion asymptotes to approximately 57 mm for wave amplitudes greater than 60 mm). In this case, the magnitude of the mean displacement appears to be independent of wave frequency. The change of mean draft can be attributed to the immersion of the upper surface and, in all cases, takes only a small number of wave cycles to develop and motion is then periodic. This is illustrated in Figure 6 where the time-varying displacement of the free surface and of the upper-surface of the float are shown for two wave amplitudes. Mid-draft float motion is nearly sinusoidal and slightly greater than the wave amplitude whereas, in the same wave conditions, the motion is not purely harmonic and is a reduced amplitude when the upper surface is immersed. For the cases shown in 6(b) and (d) it appears that the increase of mean displacment is established by the first wave crest (by $t/T_\mathrm{p} > 2.5$). During subsequent cycles, the float velocity is close to zero for almost a fifth of each wave period. This follows the instant of maximum immersion beneath each wave crest (integer values of t/T_p) and ends within the wave trough. Similar responses are observed up to 70 mm wave amplitude and the straight-sided part of the float does not emerge from the free-surface.

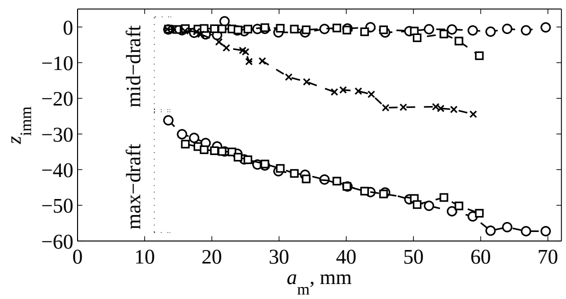

Figure 5: Variation of mean upper surface immersion with wave amplitude for incident wave frequencies of 0.688 Hz (circle; $T \sim 12$ s), 0.844 Hz (square; $T \sim 10$ s) and 1.063 Hz (cross; $T \sim 8$ s). Data is shown for both mid- and max-draft floats. Mean float position is calculated over five complete oscillations during periodic motion.

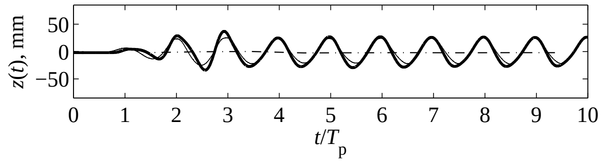

(a) Mid-draft, 21 mm amplitude

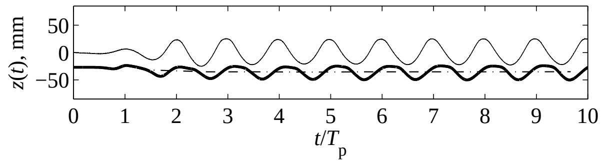

(b) Max-draft, 21 mm amplitude

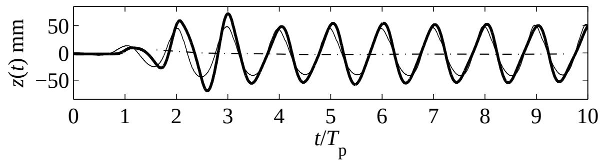

(c) Mid-draft, 40 mm amplitude

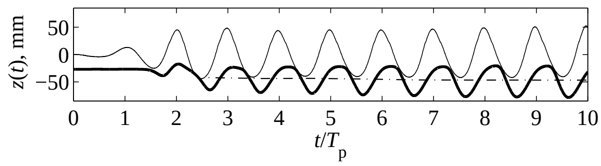

(d) Max-draft, 40 mm amplitude

Figure 6: Time-variation of displacement of upper surface of float ($z(t)$, thick solid line) due to regular waves ($\eta(t)$, thin solid line) of frequency 0.688 Hz. Mean displacement (thin dashed line) obtained over five wave cycles also shown.

4.2 Focused Waves

Several formulations have been developed which accurately describe the free-surface shape or kinematics of extremely large wave groups [15–17]. For a linear wavefield, the shape of the wave with maximum crest amplitude is identical to the autocorrelation function and consists of a short group of large amplitude waves occuring in otherwise still water. Such waves represent the design load case for fixed stuctures. It is unclear whether these waves represent the worst case loading for a near-resonant body but, in the absence of detailed information on design waves for wave devices, the maximum crest wave represents a useful benchmark. Focused events can be generated experimentally by appropriate selection of the relative phase of each regular wave component within an irregular wave-field [18, 19].

Here, focused waves for a Bretschneider spectrum (see e.g. p101 in [20]) are defined using the Edinburgh Designs OCEAN software in which phases are calculated assuming linear propagation of each component. Since wave focusing is nonlinear the calculated phases do not provide the symmetric shape expected from linear focusing alone and the resultant groups are slightly asymmetric with the trough following the crest slightly deeper than the trough preceding the crest. However, the main features of the wave are reproduced (Figure 7) and similar responses were observed with small variations of the group shape. Since our interest is in design conditions, wave groups were not considered for small wave periods. Focused wave tests were conducted with peak frequencies $f_w < 0.844$ Hz and crest amplitudes of 100 mm ($10-12$ s and 7 m crest amplitude at full-scale) for the mid- and max-draft floats only.

As observed in regular waves, float response is significantly reduced when the upper-surface is part-immersed. In all cases, maximum excursion during a wave-cycle is reduced by more than 40% and up to 60% when the upper surface is immersed in still water. For the mid-draft float, excursion is less than 70 mm during the wave cycle containing the focused crest. Maximum excursions of around 90 mm are observed during the zero-downcrossing wave cycle (trough and crest) immediately after the focused wave crest. High frequency oscillations during the trough prior to the focused crest ($-0.8 < t/T_\mathrm{p} < -0.5$, Figure 7) have a small influence on maximum float displacement shortly after the focused wave crest but do not appear to influence the maximum excursion (e.g. trough to crest) of the float. In exactly the same set of waves, maximum excursion is reduced to between 40 and 55 mm when the float draft is increased. The reduction of maximum excursion is considerably larger than the small variation of excursion due to different shapes of the focused wave so can be attributed to the different draft of the two floats.

Although maximum excursion is perhaps the most important consideration for device design, it is interesting to observe that the interval over which these maximum peak to trough motions occur are also dependent on float draft. Time-varying wave elevation, float displacement and upper-surface immersion are shown for two cases in Figure 7. Motion prior to the focused crest ($t < 0$) is similar for both floats in that the response follows the wave shape. However, the response to the first crest and trough is markedly lower for the higher draft case. As expected, maximum velocities occur during the focused wave crest although again these are roughly 40% lower for the higher draft case (time variation not shown but maximum velocities are 0.14 m/s and 0.22 m/s respectively). In all cases, the maximum absolute (negative) displacement occurs during the second trough of the wavegroup ($t \sim T_\mathrm{p}$) and, at this instant, the upper surface of the float is immersed by the same distance, approximately 25 mm, for both initial drafts. (At this position, the float upper surface is located at -60 mm below still water and the free surface at -35 mm). However, due to the larger restoring force on the mid-draft float, this attains a higher velocity (and maximum excursion) during the third wave crest ($0.8 < t/T_\mathrm{p} < 1.3$) whereas the max-draft float remains immersed throughout this third crest only gradually returning to its mean position. It is worth noting that a similar reduction of maximum excursion can be obtained by reducing the counterweight rather than increasing the float mass. Figure 7 also shows the response of a fourth configuration with float mass the same as the mid-draft float but a reduced counterweight ($m_c = 0.16$ kg) such that the immerse volume in still water is equal to that of the max-draft float (Max$^{(2)}$ in Table 1). This shows similar reduction of response for the shorter period focused wave but, for the longer period, the reduced restoring force results in greater immersion due to the focused crest. The resultant trough to peak response ($0.5 < t/T_\mathrm{p} < 1.4$) is around 60 mm; still a 30% reduction.

Although these relatively short duration focused wave groups are not necessarily the worst case design wave for an oscillating body, these findings provide some confidence that this approach to limiting float motion can be effective even in waves of extremely large crest amplitude that may occur during storm conditions. Since these wavegroups are of short duration, the mean displacement prior to the wave is the same as that in still water. If similar focused wave conditions were to occur within a regular (or irregular) wavefield, an even smaller response is likely to be observed for both floats due to an increase of mean displacement during the preceding wave cycles.

4.3 Irregular Waves

To confirm that the reduction of response observed with increased draft is not the result of periodic forcing or of the short-duration of the focused wave groups, several tests were conducted in irregular wave fields. Each wave-field was defined by a Bretschneider spectrum with significant wave heights of up to 150 mm ($H_s \sim 10$ m at full-scale). Time-varying response is illustrated for two wave periods in Figure 8 clearly indicating a reduction of response. For the case shown in Figure 8(a), maximum excursion is reduced by 60% and occurs during a different wave cycle for each float ($t/T_\mathrm{p} = 3$ for the mid-draft float and $t/T_\mathrm{p} = 6.4$ for the max-draft float). In all cases a similar reduction of response is observed and, for the mid-draft float, mean displacement is similar to that observed in large amplitude regular waves (mean offset in irregular waves approx. 10 mm). However, for the larger draft, mean displacement of -45 mm in irregular seas corresponds to the displacement in regular waves of only 35 mm amplitude. This reduction is presumably because the irregularity of the forcing allows the float to recover towards the still water position during calmer intervals.

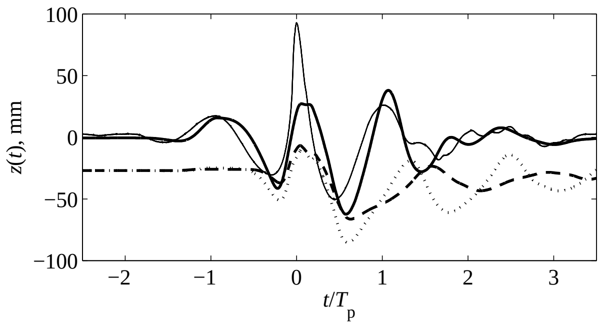

(a) Device response, $f_\mathrm{p} = 0.688$ Hz. Full scale $T_\mathrm{p} \sim 12$ s

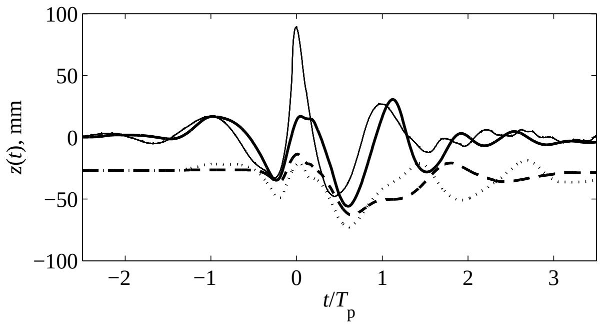

(b) Device response, $f_\mathrm{p} = 0.766$ Hz. Full scale $T_\mathrm{p} \sim 11$ s

Figure 7: Time variation of surface elevation ($\eta(t)$, thin solid line), and response of mid-draft (thick solid line) and max-draft (thick dashed line) floats during focused wave group defined by Bretschneider spectrum to give crest amplitude of 100 mm. Response of float with reduced counterweight, corresponding to Max$^{(2)}$ in Table 1, also shown (dotted line) in part (b).

5 Discussion

The purpose of this study was to determine whether the response of a float form suitable for use as a wave energy device could be limited in extreme waves by changing its draft. Our measurements show that this is possible by increasing the draft such that part of a suitably

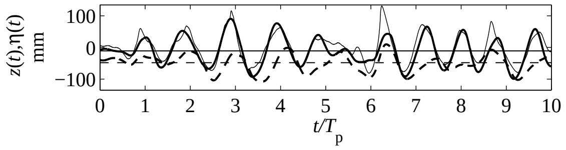

(a) Peak frequency, $f_p = 0.688$ Hz. Full scale $T_p \sim 12$ s (16)

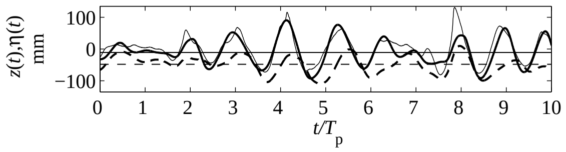

(b) Peak frequency, $f_p = 0.766$ Hz. Full scale $T_p \sim 11$ s

Figure 8: Time-varying displacement of upper surface of mid- (thick solid curve) and max- (thick dashed curve) draft floats during irregular wave (thin curve) defined by Bretschneider spectrum with significant wave height $H_s \sim 4a$ (150 mm). These waves are equivalent to full-scale peak periods of 11 and 12 s with significant wave heights of 10 m. Mean displacement of upper surface, calculated over the repeat cycle of the wave-field is also shown for mid draft (horizontal solid line) and max-draft (horizontal dashed line).

shaped upper surface of the float becomes immersed in large wave amplitudes. This results in hydrodynamic damping that limits the maximum float motion in severe seas. Limited information is available on the 3D problem of a body exiting a free surface (or oscillating beneath a free surface with large Keulegan Carpenter number) and so no attempt has been made to quantify the relative contributions of the physical processes involved at this stage. Observation suggests that during partial and shallow immersion of the upper surface, energy is dissipated through breaking and sloshing over the upper surface. Drag-type forces (i.e. in phase with velocity) on the upper surface are therefore unlikely to be significantly due to boundary layer effects. Loads will probably be dominated by flow inertia and gravity effects and would not be expected to change significantly with scale.

Boundary layer effects may be more significant on the lower surfaces of the float that remain continuously immersed (e.g. around the perimeter of the base of the float). These loads will be Reynolds number dependent and so may change with scale although limited scale dependence of the drag coefficient was observed in experimental study of a heaving float at 1:10$^{\text{th}}$ and 1:100$^{\text{th}}$ scale [21]. Although there will be differences due to geometry (particularly 3D rather than 2D flow), some insight into the relative significance of drag-type forces and added mass forces (in phase with velocity and acceleration respectively) can be obtained from the literature on water exit of a 2D body. Linear added mass theory provides a poor prediction of the cylinder loading in this idealised case [22], particularly for vertical motion in which the cylinder centroid is within 1.5 radii of the free surface. However, viscous numerical simulations (water exit of a 1 m radius horizontal cylinder in [23]) demonstrate that a nonlinear irrotational flow model (described in [24]) provides an adequate prediction of loads, at least until the free surface breaks up, suggesting that boundary layer effects are not important.

The float geometry employed comprises two cylindrical sections with the lower part of radius a and upper part of radius $a/3$ connected by a conical section of 30$^{\text{o}}$ slope. This geometry was selected such that when the waterline is within the vertical extent of the small radius cylinder, the natural period (assuming small amplitude linear response) is similar to the longer wave periods studied. The extent of the response limitation applied could be adjusted by modification of this form. Changing the profile of the upper surface would alter both the change of mass required to affect a given change of draft and may significantly influence the magnitude of forces due to breaking, sloshing and viscous effects. A reduction of the radius of the upper cylindrical section has little influence on the change of mass required to alter the draft in still water but would increase the mean displacement that occurs during response to wave loading since buoyancy force will only change by a small amount with draft. Note that, in the absence of this upper cylindrical section (the form of many heaving floats), an upward restoring force (counterweight or positive buoyancy) would be required to ensure that downward displacement is limited once the upper surface has been immersed. Conversely, a larger radius upper section would reduce the mean float displacement during loading since the increase of buoyancy force will balance the increased loads on the upper surface at a smaller draft.

6 Conclusions

Many offshore engineers are concerned with limiting the response of a floating body, particularly during extremely severe wave conditions. This is of particular importance to the designers of wave energy devices, for which finite motion constraints must be satisfied to avoid high loads as the device approaches an end-stop. One way in which the performance of heaving wave devices is tuned is to adjust the mass of the oscillating system. Such changes are difficult to achieve in practice since a large change of system mass is required to substantially alter the response amplitude. Here it is shown that the response characteristics of an axisymmetric heaving float with a conical upper surface can be significantly changed by adjusting its displaced mass and hence the water plane area of the body. It is important for the upper surface to be sloped such that a small change of mass will alter the water plane area in still water. Experimental measurements are presented of the response of a cone-topped, round-based float in several large-amplitude regular and irregular waves. By increasing the float mass (or, similarly, by increasing the ratio of displaced mass to counterweight mass), the float draft is increased causing an increase of both the natural period and of the hydrodynamic damping. Float motion can be reduced from greater than the wave height to less than 50% of the wave height by only a 10% increase of mass. Combined, these affects can be exploited to ensure that float motion remains within a specified range.

Acknowledgements

Financial support for this study was provided by the NWDA Joule Centre for Energy Research. In addition, the second author is supported by a Doctoral Training Award from the University of Manchester and an IMechE Whitworth Senior Scholarship. Discussions with Dr Frank Allison (UMIP) and the industrial partners of the Manchester Bobber Company are greatly appreciated. Aspects of this study are covered by International Application Number PCT/GB2008/003702.

References

[1] M. Previsic, R. Bedard, and G. Hagerman. Offshore wave energy conversion devices. Assessment Report E2I EPRI WP-004-US-Rev 1, EPRI, 2004.

[2] J. Falnes. *Ocean waves and oscillating systems*. Cambridge University Press, 2002.

[3] P. Nebel. Maximising the efficiency of wave-energy plant using complex-conjugate control. *Proc. IMechE Part I: J. Systems and Control Engineering*, 206:225–236, 1992.

[4] A. Babarit and A. H. Clement. Optimal latching control of a wave energy device in regular and irregular waves. *Applied Ocean Research*, 28:77–91, 2006.

[5] A. F. de O. Falcão. Phase control through load control of oscillating-body wave energy converters with hydraulic PTO system. *Ocean Engineering*, 35:358–366, 2008.

[6] J. Falnes. A review of wave-energy extraction. *Marine Structures*, 20:185–201, 2007.

[7] M. Alves, H. Traylor, and A. Sarmento. Hydrodynamic optimization of a wave energy converter using a heave motion buoy. In *Proc. 7^{th} European Wave and Tidal Energy Conference (EWTEC)*, Porto, Portugal, 2007.

[8] Massachusetts 02467-2504 WAMIT Inc., Chestnut Hill. *WAMIT User Manual*, 2008.

[9] G. Thomas. The theory behind the conversion of ocean wave energy: a review. In J. Cruz, editor, *Ocean Wave Energy: Current Status and Future Perspectives*. Springer-Verlag, 2008.

[10] R. Taghipour, T. Perez, and T. Moan. Hybrid frequency-time domain models for dynamic response analysis of marine structures. *Ocean Engineering*, 35(7):685–705, 2008.

[11] Fugro GEOS. Wind and wave frequency distributions for sites around the british isles. Offshore Technology Report 2001/30, Health and Safety Executive, 2001.

[12] M. A. Srokosz. Some relations for a body in a canal with an application to wave power absorption. *Journal of Fluid Mechanics*, 99(1):145–162, 1980.

[13] T. Bjarte-Larsson, J. Falnes, and T. Moan. Comparison of results from time-domain simulations and model tests of a water-pumping wave-power unit. In *Proc. 16^{th} Offshore and Polar Eng. Conf. (ISOPE)*, San Francisco, CA, USA, 2006.

[14] M. Vantorre, R. Banasiak, and R. Verhoeven. Modelling of hydraulic performance and wave energy extraction by a point absorber in heave. *Applied Ocean Research*, 26:61–72, 2004.

[15] P. S. Tromans, A. Anatuak, and P. Hagermeijer. A new model for the kinematics of large ocean waves - application as a design wave. In *Proc. 1^{st} Offshore and Polar Eng. Conf. (ISOPE)*, Edinburgh, UK, 1991.

[16] G. F. Clauss. Dramas of the sea: episodic waves and their impact on offshore structures. *Applied Ocean Research*, 24:147–161, 2002.

[17] C. T. Stansberg, O. T. Gudmestad, and S. K. Haver. Kinematics under extreme waves. *Journal of Offshore Mechanics and Arctic Engineering*, 130:021010–1, 2008.

[18] T. E. Baldock, C. Swan, and P. H. Taylor. A laboratory study of nonlinear surface waves on water. *Phil Trans R. Soc. Lond. A*, 354:649–676, 1996.

[19] D. Rogers and G. Bolton King. Wave generation using ocean and wave. Technical Report Version 3.62, Edinburgh Designs Ltd, 1997.

[20] M. J. Tucker and E. G. Pitt. *Waves in Ocean Engineering*. Ocean Engineering Series. Elsevier, 2001.

[21] P. K. Stansby. Robust wave energy device evaluation and design. Technical Report 2004-10-18, The Carbon Trust, 2004.

[22] M. Greenhow and Y. Li. Added masses for circular cylinders near or penetrating fluid boundaries - review, extension and application to water-entry, -exit and slamming. *Ocean Engineering*, 14(4):325–348, 1987.

[23] P. Lin. A fixed-grid model for simulation of a moving body in free-surface flows. *Computers and Fluids*, 36:549–561, 2007.

[24] M. Greenhow and S. Moyo. Water-entry and -exit of horizontal circular cylinders. *Phil Trans Roy Soc Lond. A.*, 355:551–563, 1997.